Patterns of Inflammation in Experimental Autoimmune Uveitis and Their Correlation to Optical Coherence Tomography Findings in Human Uveitis

Benedikt Schworm *, Tarek Ghannoum , Stephan Thurau , Gerhild Wildner *

Posted Date: 18 December 2025

doi: 10.20944/preprints202512.1701.v1

Keywords: uveitis; chorioretinitis; vasculitis; experimental autoimmune uveitis; immunohistochemistry; oct imaging; molecular pathomechanims

 doi:10.20944/preprints202512.1701.v1

Article

Patterns of Inflammation in Experimental Autoimmune Uveitis and Their Correlation to Optical Coherence Tomography Findings in Human Uveitis

Benedikt Schworm *,†, Tarek Ghannoum †, Stephan Thurau and Gerhild Wildner *

Department of Ophthalmology, University Hospital, LMU Munich, Mathildenstr. 8, 80336 Munich, Germany

* Correspondence: benedikt.schworm@med.uni-muenchen.de (B.S.); gerhild.wildner@med.uni-muenchen.de (G.W.)

† These authors contributed equally to this work, shared first authorship.

Abstract

Background/Objective: Experimental autoimmune uveitis (EAU) in rats is a model of human uveitis that is pivotal for understanding the immunological mechanisms of the disease and developing therapies. In humans, optical coherence tomography (OCT) enables in vivo detection of characteristic findings in active uveitis, as well as sequelae of inflammation. This study aimed to correlate OCT findings in uveitis patients with retinal histologies from two rat models of experimental autoimmune uveitis caused by T cells with different autoantigen specificities and gene expression patterns, as well as well-known underlying immunological pathomechanisms. **Methods:** Patients with various noninfectious uveitis subtypes were imaged using ultrawidefield swept-source or conventional OCT. Histological cryosections from rat eyes with experimental autoimmune uveitis were stained for T cell and/or macrophage markers. **Results:** Typical human OCT findings were reproduced in the experimental animal model. Hyperreflective signals observed on OCT corresponded to lymphocyte infiltration in histological sections, which was typically found in perivascular regions (vasculitis), the posterior hyaloid (snowballs), and retinal infiltrations by lymphocytes and macrophages through the retinal pigment epithelium. **Conclusions:** Comparing in vivo OCT imaging of human uveitis with corresponding histologies from rat models improves our understanding of the type of inflammation, the extent of tissue destruction, and the immunopathogenesis.

Keywords: uveitis; chorioretinitis; vasculitis; experimental autoimmune uveitis; immunohistochemistry; oct imaging; molecular pathomechanims

1. Introduction

Uveitis is the collective term for inflammatory diseases of the intraocular structures. Uveitis is classified as anterior, intermediate, or posterior based on the primary site of inflammation. This condition can range from mild to severe, threatening vision. Patients with autoimmune uveitis often require continuous immunosuppressive therapy and regular monitoring of disease activity through ophthalmological assessments, such as slit-lamp examinations and indirect fundoscopies.[1].

Over the past two decades, modern imaging modalities have increasingly complemented the clinical evaluation of patients with uveitis. Among these modalities, optical coherence tomography (OCT) has proven particularly valuable for visualizing retinal structural changes. Recently, OCT was incorporated into the minimum imaging requirements for various forms of non-infectious posterior uveitis [2]. Currently, its application mainly focuses on the posterior pole of the eye, particularly the macular region and the optic nerve head.

 doi:10.20944/preprints202512.1701.v1

With the advent of ultrawidefield imaging devices, however, peripheral retinal structures can now be visualized. These structures have thus far been poorly characterized in uveitis. Many imaging findings appear to correlate with active inflammation, while others are indicative of chronic disease, structural damage and loss of retinal tissue. Since uveitis is an inflammatory disorder, several of these imaging features are likely due to immune cell accumulation and/or migration. Direct histological verification in humans is not feasible, because ocular biopsies pose a risk of vision loss.

Despite the increased resolution of OCT scans in the recent years, many details remain hidden and we only have a general idea of the extent of retinal infiltration and destruction. Furthermore, we cannot determine the type of infiltrating cells. Therefore, we examined histological sections of rat eyes with experimental autoimmune uveitis (EAU) to gain a more detailed understanding of the cell types and the sites of retinal invasion. Correlating with the autoantigen specificities of the experimental models allows us to speculate about the expression, degradation and presentation of the respective autoantigens. The gene expression profiles of the autoreactive T cells in rat models explain certain sequelae such as chorioretinal neovascularization and relapses [3–7].

Experimentally induced autoimmune uveitis (EAU) in animals demonstrates disease patterns that closely resemble those observed in humans. EAU in Lewis rats has been thoroughly investigated with respect to histological images of retinal infiltration and destruction, and immune mechanisms. The two major autoantigens used to induce EAU in Lewis rats are retinal S-antigen (S-Ag, arrestin) and interphotoreceptor retinoid-binding protein (IRBP), as well as peptides representing their most pathogenic epitopes [7].

The respective ocular autoantigens for human uveitis remain unknown. Antibody and T-cell responses to S-antigen, IRBP, and some peptides have been demonstrated; however, the full spectrum of ocular autoimmune responses remains unclear [8,9]. Nevertheless, EAU in rats serves as a valuable model for human autoimmune uveitis. It has been used to detect pathomechanisms and test new potential therapies for uveitis. Finally, we have found striking similarities between retinal optical coherence tomography (OCT) images from uveitis patients and histological retinal images from rat EAU [10–14].

The S-Ag peptide PDSAg induces a chronic, clinically monophasic uveitis with formation of chorioretinal neovascularization due to the VEGF production of the autoreactive T cells [6]. In contrast, immunization of rats with the IRBP-peptide R14 leads to a spontaneously relapsing disease, fueled by the higher IFN-γ production of R14-specific T cells [3,4,6,13]. Moreover, in S-Ag- and PDSAg-induced uveitis we found that T cells and inflammatory cells are mainly recruited from the choroid through the RPE. This suggests that the RPE or other antigen-presenting cells like macrophages located within the choroid, present the autoantigen. In contrast, IRBP/R14-induced EAU shows infiltration via retinal capillaries, which usually leaves the RPE intact [15]. in human uveitis the antigen specificities of the autoimmune responses and the types of lymphocytes and leukocytes that drive the inflammation and are unknown.

Not only do autoreactive T cells recognize different retinal autoantigen epitopes; they also differ in cytokine and chemokine secretion and expression of various surface receptors. This has been demonstrated in rat models with autoreactive T cells specific for peptides from S-Ag (PDSAg) and IRBP (R14) [4,5,13]. Depending on their cytokine profile, they can recruit different inflammatory cells, such as monocytes/macrophages or granulocytes. This results in either granulomatous/nodular (macrophages) or non-granulomatous (neutrophil granulocytes) ocular inflammation. In rat EAU, the predominant infiltrating leukocyte populations are monocytes/macrophages; however, we also observe granulocytes. Thus, we cannot distinguish between granulomatous and non-granulomatous uveitis types in the rat model.

Nevertheless, by comparing human OCT scans from various posterior uveitis entities with sections from rat eyes with EAU and immunohistochemical staining, we found striking similarities between human and experimental uveitis. This helps us better understand the fine structure of inflammatory signs in retina and vitreous and characteristics of tissue destruction.

 doi:10.20944/preprints202512.1701.v1

2. Materials and Methods

2.1. Patient Recruitment and Characteristics

Eight patients with different types of uveitis from our outpatient department underwent diagnostic OCT imaging of the retina. Basic clinical data was collected from each patient and brief case descriptions are found in the figure legends, respectively. Ethics approval and informed consent was obtained for all patient data (see section "Institutional Review Board Statement" below).

2.2. OCT Imaging

Spectral-domain OCT imaging was performed on a Heidelberg Spectralis device (Heidelberg Engineering, Heidelberg, Germany). Macular volume scans were recorded with the following settings: 20°x20° (5.9x5.9mm), 49 horizontal B-scans, 18≤ART≤30. Swept-Source ultrawidefield imaging was performed with an Intalight® DREAM OCT™ (SVision Imaging Ltd., Jianxi District, Henan, China). Images were acquired in a star shaped scan pattern of 18 radial B scans centered to the fovea (scan length 26mm, depth 6,3mm).

2.3. Histological Case Selection Process and Analysis

Our existing research database of routinely prepared histological images for histolocial scoring of EAU from previous experiments was re-examined and newly analyzed with particular focus on cell types, inflammation sites, inflammatory patterns, and clinical transferability in terms of their correspondence to human OCT findings. The histological pictures have not been published.

2.4. Induction of Experimental Uveitis

Male and female albino Lewis rats were either obtained from the Central Institute for Laboratory Animal Breeding (Hannover, Germany), RCC (Basel, Switzerland), Janvier (Le Genest St. Isle, France) or bred in our own colony and maintained under specific pathogen-free conditions with water and food ad libitum and used for experiments at the age of 6–8 weeks.

The rats were immunized subcutaneously in both contralateral hind legs with a total of 15 µg of retinal S-Ag peptide PDSAg (amino acids 342-355, FLGELTSSEVATEV (1)), or 15 µg of IRBP-peptide R14 (amino acids 1169-1191, PTARSVGAADGSSWEGVGVVPDV). The peptides were emulsified in an equal volume of CFA containing 2.5 mg/ml of Mycobacterium tuberculosis strain H37Ra (DIFCO, Hedinger, Stuttgart, Germany) and phosphate-buffered saline. IRBP was prepared from bovine eyes as described (3), and its purity was controlled by gel electrophoresis. The peptides PDSAg and R14 were purchased from Biotrend, Cologne). No B. pertussis or pertussis toxin was used as an additional adjuvant. A total volume of 200 µl of emulsion was injected subcutaneously into each hind leg.

2.5. Immunohistochemistry

Eyes were collected for histology after the termination of the experiments between days 21 and 24 post immunization. The enucleated eyes were snap frozen in Tissue Tec OCT compound (Sakura Finetek, Torrance, CA) in methylbutane at -70°C. Frozen sections (8 µm) were layered on poly-L-lysine (SIGMA, Deisenhofen, Germany) precoated slides, fixed in ice-cold acetone, and air-dried. Then, mouse anti-rat monoclonal antibodies specific for CD4 (W3/25, provided by Th. Hünig, Würzburg, Germany), TCR-αβ (R73, provided by Th. Hünig, Würzburg, Germany), or ED1 (monocytes/macrophages, Biozol, Eching, Germany) were added for 1 h. The slides were washed twice in Tris/HCl (pH 7.5) before adding the secondary antibody, F(ab') rat anti-mouse Ig (1:50, Dianova, Hamburg, Germany). For staining of Met-RANTES, Met-RANTES or PBS (control) were added for 1 h at RT, after washing with Tris buffer mouse anti-human RANTES antibody VL2 (gift from Peter J. Nelson) was added for another hour before staining was continued as follows: the slides were washed once more with Tris buffer, and then an alkaline phosphatase-anti-alkaline phosphatase (APAAP) complex (1:80, Dianova) was added. We used New Fuchsin as the substrate, as described

 doi:10.20944/preprints202512.1701.v1

(4). In some cases, the immunohistochemical staining step was omitted, and the slides were only counterstained with hematoxylin. The slides were mounted with glycerol gelatin and imaged with a Zeiss Axioskop 2plus (Carl Zeiss). Photographs were taken with a Sony CyberShot DSC-S70 3.3MP digital camera.

3. Results

3.1. Different Sites of Ocular Infiltration by Inflammatory Cells

In rats S-Ag-peptide PDSAg-induced EAU generally shows a retinal infiltration of cells via the choroid and RPE, resulting in RPE and adjacent retinal layer destruction. Additionally, we observed new vessel growth from the choroid, similar to that seen in some patients with choroiditis. In contrast, R14-induced uveitis shows cellular infiltration primarily via the retinal vessels (in the outer and inner plexiform layers). This results in destruction of the retinal architecture while leaving the RPE largely intact [15]. This inflammation patter resembles human intermediate uveitis with regard to vitreous infiltrates and peripheral periphlebitis.

Recently, we have demonstrated a reactivation of previously inflamed retinal foci in the rat model in which GFP+ T cells preferentially invaded sites of prior tissue destruction, causing relapses [7].

The infiltration routes of immune cells differ between the two types of rat EAU: PDSAg-specific T cells preferentially infiltrate via the RPE, while R14-specific T cells invade via the retinal vessels (e. g. in the outer plexiform layer) [15]. Staining rat retina sections with Met-RANTES revealed its binding to some infiltrating cells (Figure 1A, asterisks) and to the basolateral site of the RPE (Figure 1A, arrows).

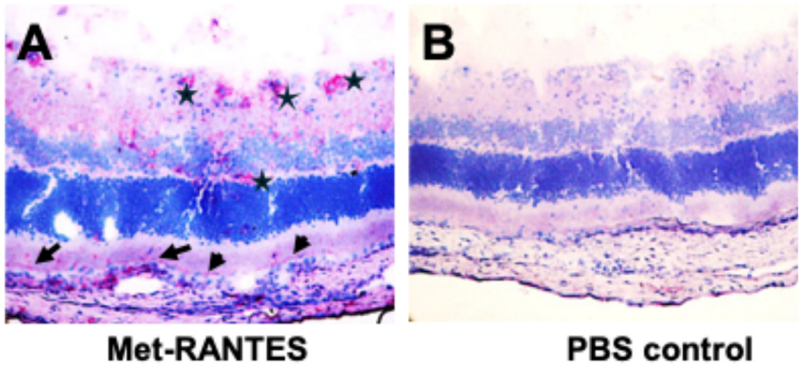

Figure 1. (A): Rat eye with mild R14-induced EAU stained for binding of Met-RANTES, visualized with anti-huRANTES antibody VL2 (asterisks and arrow). (B): PBS added instead of MetRANTES. Endogenous rat RANTES is not detected with VL2. MetRANTES binds to CCR1 and/or CCR5 of RPE (arrows) and infiltrating cells (A, asterisks, red staining).

3.2. Infiltration of Inflammatory Cells Via the Choroid and the Outer Blood-Retina Barrier

Several uveitis entities originate in the choroid with inflammatory infiltrates spreading to the retina via the RPE. Figure 1A-C shows OCT scans of a patient with multifocal choroiditis. The stages that acute lesions in multifocal choroiditis undergo on OCT have been previously described [16]: First, small nodular lesions appear at the level of the RPE, causing an upward bulge that resembles a small pigment epithelium detachment. Then, hyperreflective infiltrates expand through the RPE into the outer retina leading to a disorganization of the retinal layer architecture of varying severity. With successful treatment, these disorganizations, as well as the hyperreflective infiltrates of the retina, disappear. However, a certain degree of RPE and outer retinal atrophy remains, leaving behind the punched-out focal atrophic lesions that can be seen on fundoscopy.

 doi:10.20944/preprints202512.1701.v1

Histologies of rat EAU eyes demonstrate that immune cell infiltration is focal and not evenly distributed across the choroid-RPE interface (Figure 2D, E F). An accumulation of CD4+ T helper cells and monocytes/macrophages occurs in the choroid just below the infiltration site. As seen in Figure 2E only few CD4+ cell invade the photoreceptor layer, the other, unstained cells may be CD8+ T cells, B cells, NK cells and granulocytes. Interestingly, despite the massive infiltration the RPE monolayer remains intact for an extended peroiod (Figure 2D, E), but is ultimately destroyed by continuing inflammation. Similar findings can be seen in the OCT scans, which show hyperreflectivity in the choroid under the lesions (Figure 2B, C). Moreover, single infiltrating cells can be found within the photoreceptor and the nuclear layers (Figure 2D-F), indicating wider inflammation spreading beyond the obvious foci. These small, hyperreflective irregularities, which are also referred to as hyperreflective foci may be represented in the OCT scans [17] (Figure 2B and C, right panels).

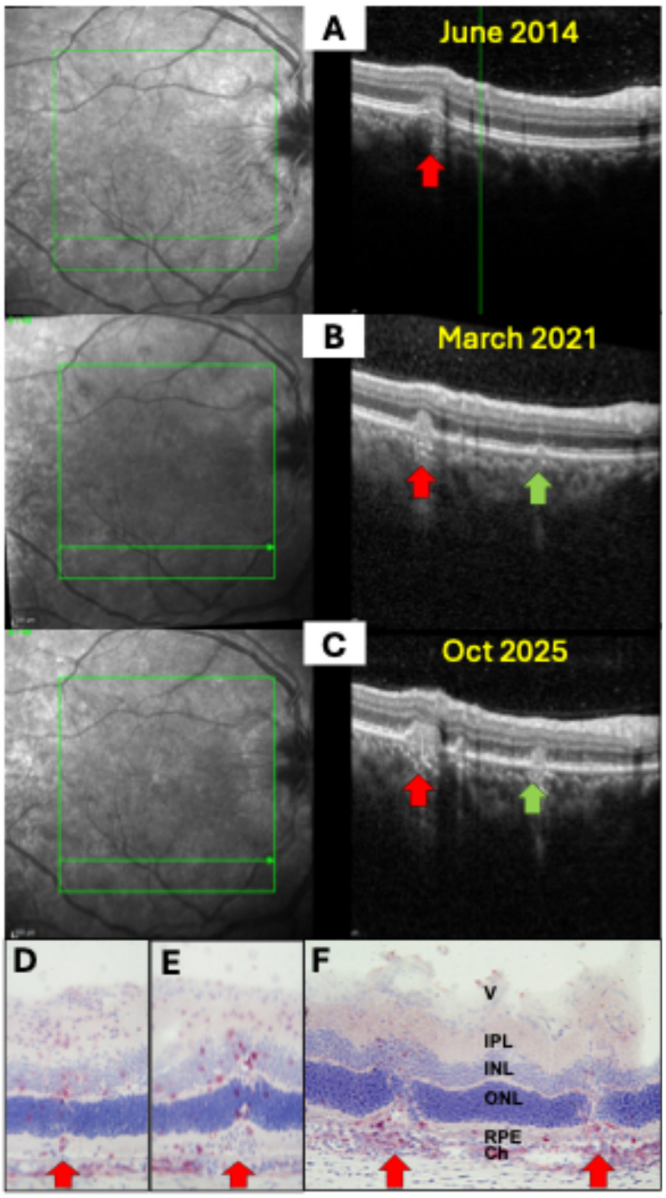

Figure 2. SD-OCT images of a 34-year-old female patient with multifocal choroiditis and progressing lesions over 11 years (A-C) with infiltration from the choroid with destruction of the RPE and the outer nuclear layer (red and green arrows). The left panel shows the confocal scanning laser ophthalmoscope (cSLO) images with the OCT scan location indicate by a green line. The scan location was identical in all three images. Similar pictures are obtained from PDSAg-induced rat EAU (D-F), with CD4+ T helper cells and macrophages (red staining) infiltrating the retina via the RPE with focal destruction of the superincumbent layers of the retina and the RPE

 doi:10.20944/preprints202512.1701.v1

(F). While the RPE is still intact in early stages in both human uveitis and rat EAU (A, D, E), focal destruction of the RPE layer increases with progressive disease (B, C, F).

Chorioretinal lesions are sometimes followed by the uncontrolled sprouting of new vessels from the choriocapillaris into the retina. This results in focal destruction of the RPE layer, as seen in punctate inner choroidopathy (PIC) (Figure 3). Previously, it was believed that VEGF originated from stressed RPE cells or choroidal macrophages. However, we demonstrated that T cells can secrete VEGF, inducing CNVs (choroidal neovascularization). PDSAg-, but not R14-specific T cells in the rat model produce VEGF and thus cause growth of new vessels (Figure 3C-F), which can be observed after the peak of inflammation. They CNVs increase in number and intensity even after the resolution of the clinically visible inflammation, because some autoreactive, VEGF-secreting T cells remain within the retina for some weeks in rat EAU [7]. CNV formation can be prevented or alleviated by suppressing the T cells in EAU (Figure 3D and [6]). In the patient shown here regression of CNVs was induced by intraocular injection of the anti-VEGF antibody ranibizumab (Figure 3B).

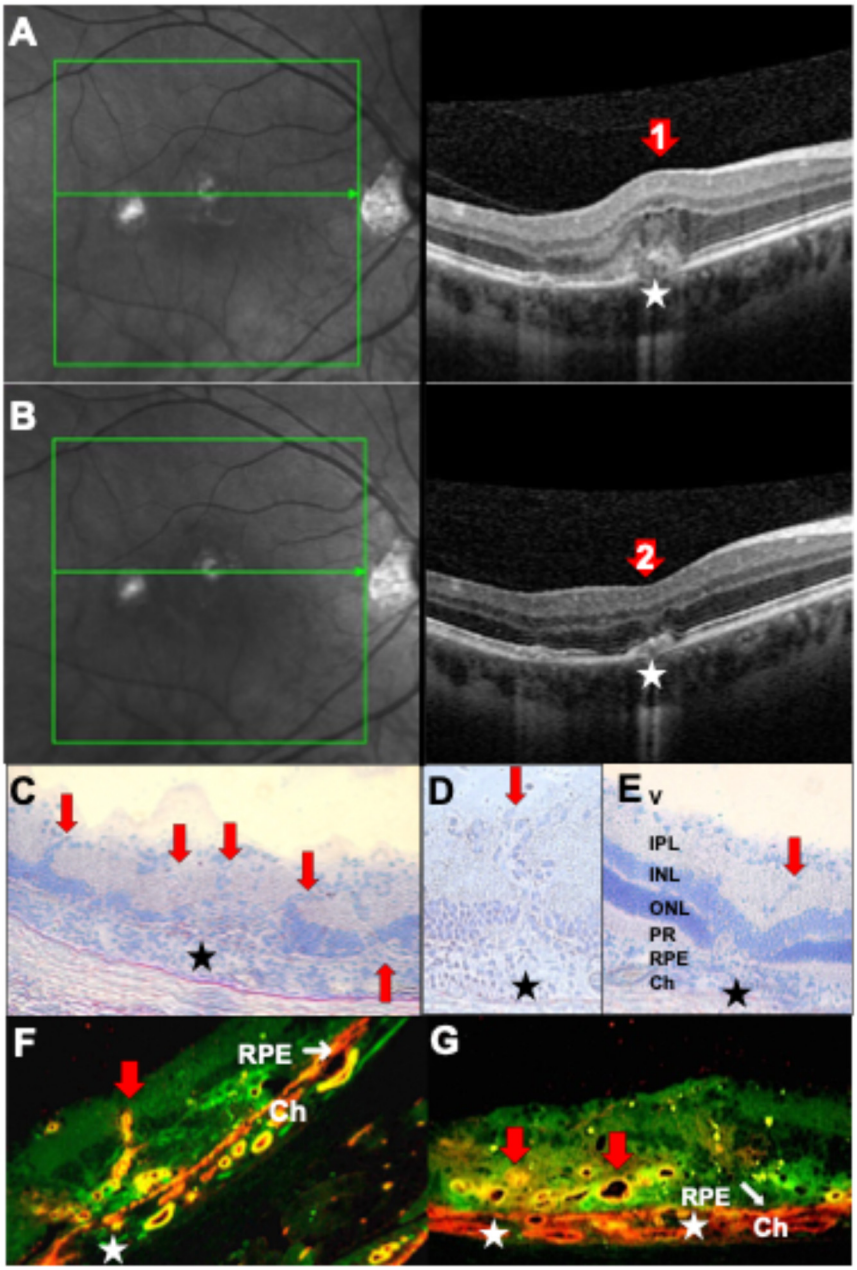

Figure 3. Choroidal neovascularizations (CNV) in uveitis. (A, B) SD-OCT B scans (right) and corresponding cSLO images (left) of a 31-year-old male patient with PIC and secondary choroidal neovascularization. (A)

 doi:10.20944/preprints202512.1701.v1

Active CNV with thickening of the retinal, cystoid hyporeflective spaces indicating fluid accumulation in the Henle fiber layer and inner nuclear layer and subretinal hyperreflective lesions with disruption of the RPE (red arrow 1). (B) The same scan region 4 weeks after one intraretinal injection of ranibizumab (red arrow 2). (C, D) Rat retina histology (cryosection, hematoxylin-stained) of PDSAg-induced EAU with severe retinal destruction extending to the inner nuclear layer and new vessels sprouting from the choroid to the ganglion cell layer (red arrows). (E) Same EAU induction as in C and D, but rat treated with systemic cyclosporin A from onset of uveitis to the end of the experiment at day 39. Cyclosporin A suppressed T cells and thus their VEGF production followed by a suppression of CNV. Asterisks mark focal destruction of the RPE and underlying choroidal infiltration. V: vitreous, IPL: inner plexiform layer, INL: inner nuclear layer, ONL: outer nuclear layer, PR: photoreceptors, RPE: retinal pigment epithelium, Ch: choroid. (F, G): Rat retina histologies with CNV and staining for CD31 (red) and CD146 (green), overlay of both stainings is shown. Red arrows mark CNVs (F) longitudinal sections, (G) cross sections through the blood vessels), white asterisks: focal RPE destruction. Ch: choroid.

In addition to the small, focal lesions shown in Figure 2 choroiditis can also result in broader atrophic lesions that affect multiple layers of the retina (Figure 4), destroying the RPE and, consequently, the outer blood-retina barrier. The OCT scan (Figure 4A) shows that the peripheral lesion extends to the inner nuclear layer. This is also seen in rat EAU in Figure 4B and C, where infiltrating macrophages (ED1 staining, Figure 4B) and T cells (staining for $\alpha\beta$ T cell receptor, Figure 4C) are visualized separately. This demonstrates the relationship between a small number of immigrating T cells and many infiltrating macrophages. Interestingly, despite the complete destruction of the photoreceptor outer segments, the RPE layer remains mostly intact.

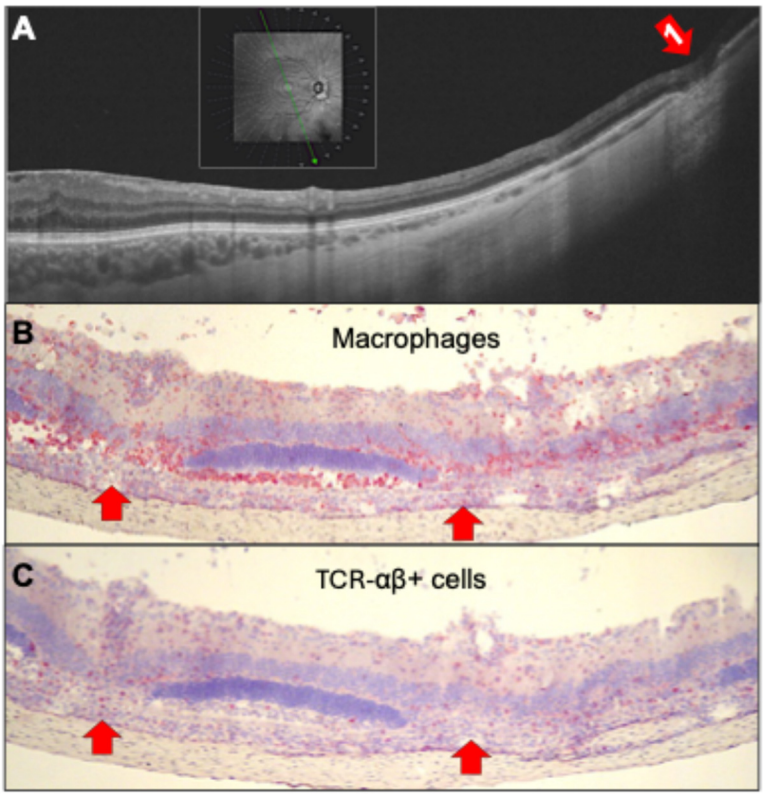

Figure 4. (A) Ultrawidefield swept-source OCT B-scan of the right eye of a 52-year-old female patient with multifocal choroiditis showing peripheral atrophy of the choroid, the RPE and outer retinal layers (red arrow 1). (B, C) In acute inflammation rat histology shows massive infiltration of inflammatory macrophages (B) and fewer TCR-$\alpha\beta$+ T cells (C), red staining, and severe destruction of outer retinal layers, and some focal lesions of the RPE (red arrows), which can be detected in human OCT as residual loss of outer retina and RPE (A, red arrow), while active inflammation has subsided. In rat EAU perivascular inflammation of retinal vessels in the ganglion cell layer can be observed in addition. (B, C) R14-immunized.

 doi:10.20944/preprints202512.1701.v1

3.3. Chorioretinitis: Infiltration Via Retinal Vessels (Inner Blood-Retina Barrier) and Choroidal Inflammation

As with rat EAU, in which retinal vasculitis and infiltration via the choroid and RPE can be observed in PDSAg-induced EAU, there are also patients with chorioretinitis, showing both inflammation of the choroid and retinal vessels.

One patient with intermediate uveitis (Figure 5A) had two retinal lesions that originated from retinal vessels and resulted in extended destruction of retinal layers. Although the Figure 5: (A) Radial ultrawidefield SS-OCT B scan of the right eye of a 69-year-old male patient with chronic intermediate uveitis and peripheral vasculitis under immunosuppression with ciclosporine. Perivascular hyperreflective infiltrates with thickening and partial disruption of the inner retinal layers (red arrows 1 and 2) and a hyperreflective transretinal infiltrate with discontinuation of the outer retinal layers (below red arrow 1) indicate residual inflammatory activity. Yellow asterisks mark the optic nerve head. (B, C) Similar features can be found in rat EAU retinas after PDSAg-immunization with focal destruction of outer and inner nuclear layers (red arrows corresponding to the respective lesions in A). Histologies reveal destruction of photoreceptor outer segments and outer retinal layers with inflammation was clinically graded as inactive on the day the image was acquired, OCT revealed perivascular hyperreflective infiltrates with thickening and partial disruption of the inner retinal layers (red arrows 1 and 2) and a hyperreflective transretinal infiltrate with discontinuation of the outer retinal layers (below red arrow 1), indicating residual inflammatory activity. Similar retinal destructions are seen in the rat sections in Figures 5B and C. Lesion No. 2 in the OCT scan (Figure 5A) appears to spread from retinal capillaries in the outer plexiform layer, as seen in the rat histology of Figure 5C.

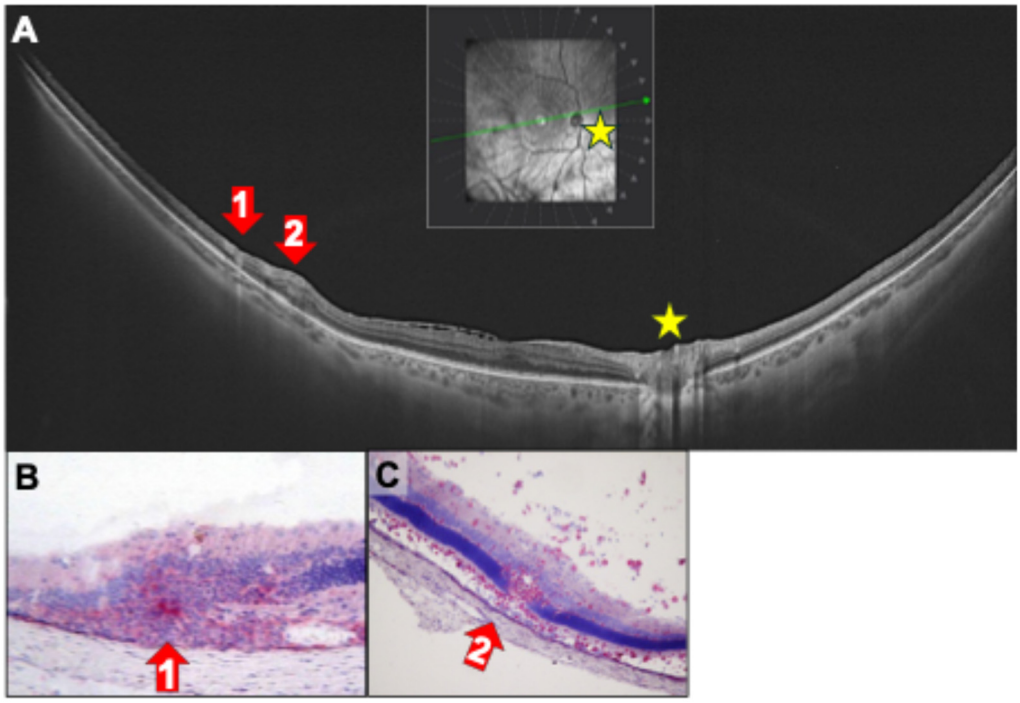

Figure 5. (A) Radial ultrawidefield SS-OCT B scan of the right eye of a 69 year old male patient with chronic intermediate uveitis and peripheral vasculitis under immunosuppression with ciclosporine. Even though the inflammation was clinically graded as inactive at the day of image aquisition, perivascular hyperreflective infiltrates with thickening and partial disruption of the inner retinal layers (red arrows 1 and 2) and a hyperreflective transretinal infiltrate with discontinuation of the outer retinal layers (below red arrow 1) indicate residual inflammatory activity. Yellow asterisks mark the optic nerve head. (B/C) Similar features can be found in rat EAU retinas after PDSAg-immunization with focal destruction of outer and inner nuclear layers (red arrows corresonding to the respective lesions in (A). Histologies reveal destruction of photoreceptor outer segments and outer retinal layers with infiltration of CD4+ T cells and macrophages (red staining).

 doi:10.20944/preprints202512.1701.v1

Despite treatment with a combination of adalimumab and mycophenolate-mofetil, a patient with birdshot chorioretinopathy revealed peripheral vasculitis with additional perivascular swelling (Figure 6A). The thickened venules correspond to mild exudation in fluorescein angiography (not shown) and were clinically graded as mild vasculitis. Corresponding rat histologies are shown in Figure 6B and C). In the vasculitic areas, the outer retinal layers appear thinned and granular. The macula was unaffected (Figure 6A).

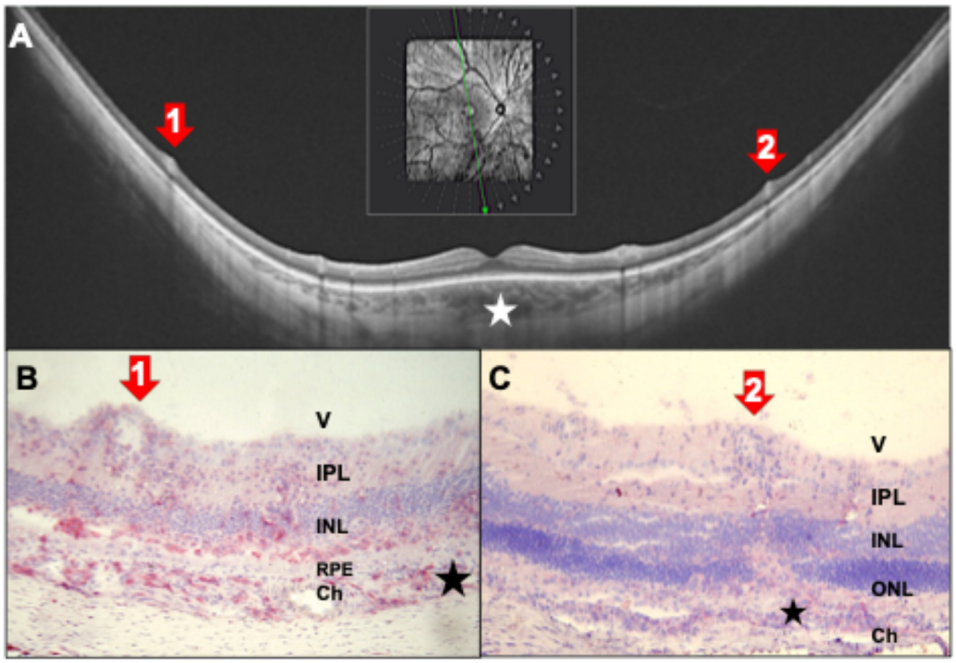

Figure 6. (A) Ultrawidefield SS-OCT B scan of a 47-year-old female patient with birdshot chorioretinopathy (BCR) and myopia with vasculitis and perivascular swelling (red arrow 1 and 2). Red arrows 1 and 2 indicate the location of thickened peripheral venules. (B, C) In rat EAU perivascular inflammation of a retinal vessel (red arrows) with inflammatory cell infiltrate (B: red staining of CD4+ cells) and total destruction of photoreceptors (outer segments and outer nuclear layer) is visible (B). (B, C) Choroidal swelling and focal destruction of the RPE (black asterisks). V: vitreous, IPL: inner plexiform layer, INL: inner nuclear layer, ONL: outer nuclear layer, PR: photoreceptors, RPE: retinal pigment epithelium, Ch: choroid. (B) R14-immunized; (C) PDSAg-immunized.

3.4. Inflammation of the Retinal Vessels and Infiltration of the Vitreous

Most patients with intermediate uveitis suffer from vasculitis of the retinal vessels and cellular infiltration of the vitreous. This leads to floaters and an epiretinal accumulation of inflammatory cells that present as "snowballs" and "snowbanks" [18].

Figure 7A shows the OCT scan of a patient with intermediate uveitis, vasculitis and a snowball. In addition, cells can be detected in the vitreous. A similar pattern is seen in rat EAU (Figure 7B), which exhibits retinal vasculitis and a snowball (Figure 7C).

 doi:10.20944/preprints202512.1701.v1

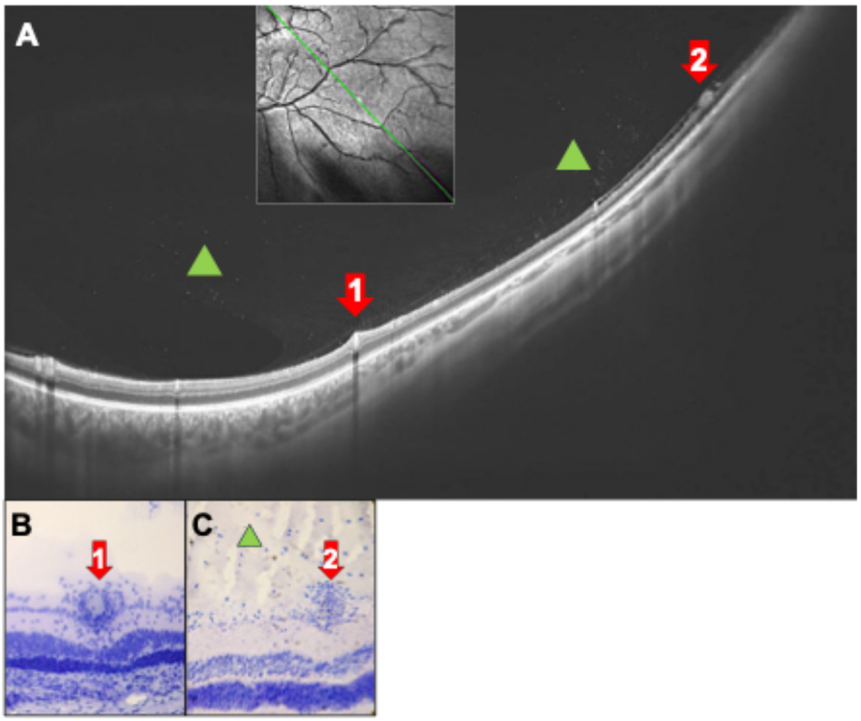

Figure 7. (A) OCT scan of a 32-year-old patient with intermediate uveitis and peripheral vasculitis. Infiltration of the vitreous by inflammatory cells (green triangles). Red arrows 1: Section through retinal vein with perivascular sheathing. Red arrow 2: An epiretinal snowball formed by a massive accumulation of inflammatory cells. See also corresponding rat histology (B, C) of a rat eye after PDSAg-immunization. Hematoxylin staining only.

Another patient with intermediate uveitis presented with peripheral snowballs and snowbanks, vitreous infiltrates and papillitis (Figure 8). Histologies from EAU rat eyes display tight accumulations of inflammatory cells within or adjacent to the ganglion cell layer, either round (snowball) or elongated (snowbank) and represent the hyperreflective structures seen in OCT (Figure 8A, C, D). The cellular infiltration of the vitreous at the optic nerve, as seen in the OCT scan (Figure 8B) originates from the inflamed central retinal vein, as demonstrated in the rat histologies (Figure 8E, F).

 doi:10.20944/preprints202512.1701.v1

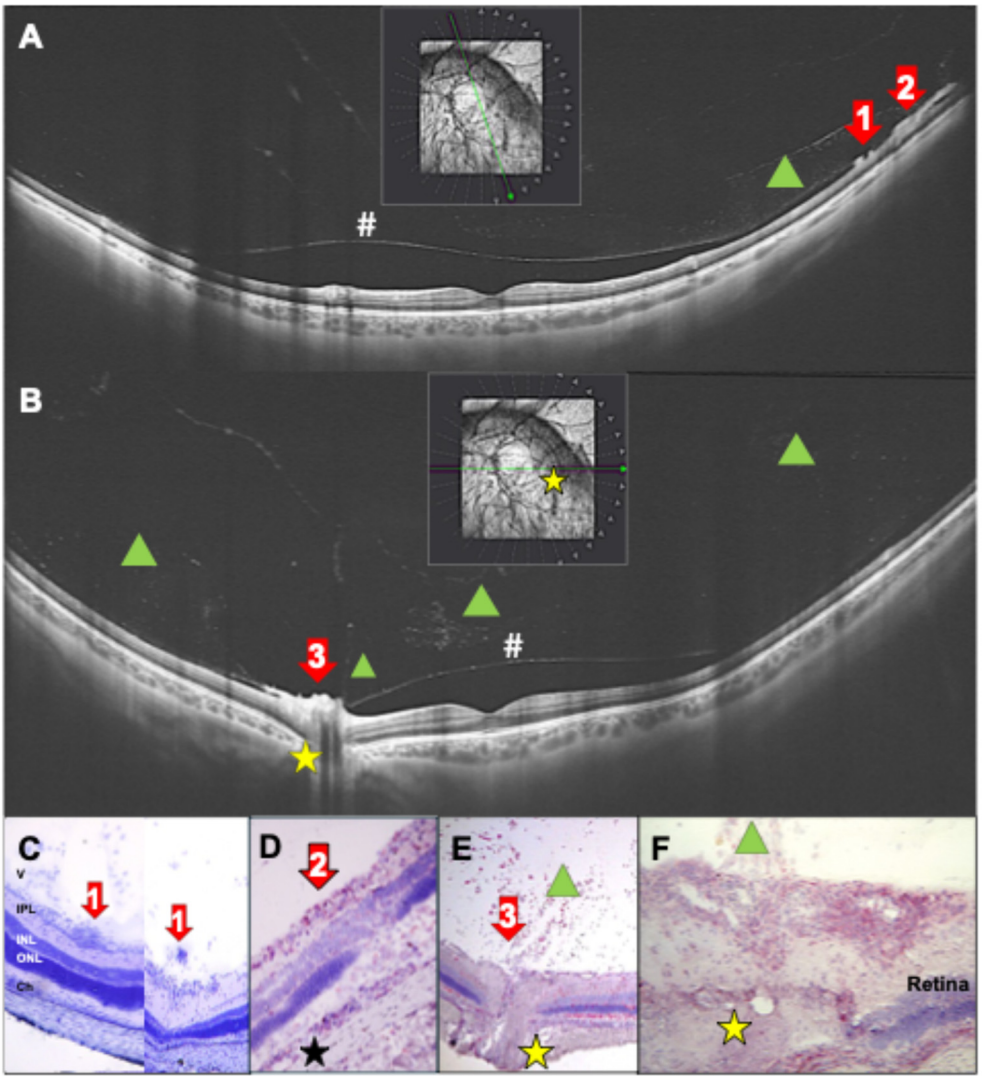

Figure 8. (A) Ultrawidefield SS-OCT scans show inferior snowballs and snowbanks (red arrows 1,2) in a 31-year-old female patient with newly diagnosed untreated intermediate uveitis. B: Same patient with papillitis (red arrow 3; yellow asterisks mark the optic nerve head) and cells infiltrating the vitreous (green triangles). Posterior hyaloid is detached (#). (C) Rat histology with snowball (red arrow 1) and snowbank (red arrow 2) at the vitreous membrane. (D) Rat retina with late-stage EAU, tight accumulation of inflammatory cells in the ganglion cell layer (snowbank, red arrow 1) and focal retinal destruction. Black asterisk marks focal destructions of the RPE. (E, F) Papillitis (red arrow 3) with CD4+ cells infiltrating the vitreous from the papilla (green triangle). Photoreceptors are destroyed and infiltrated with inflammatory cells (red staining). (F) Magnification of the optic nerve head with inflamed central retinal veins and cellular exudates. (C) hematoxylin staining only, (D-F) CD4-staining in red. V: vitreous, IPL: inner plexiform layer, INL: inner nuclear layer, ONL: outer nuclear layer, PR: photoreceptors, RPE: retinal pigment epithelium, Ch: choroid. (C, D) PDSAg-immunized; (E, F) IRBP-immunized.

The typical findings of intermediate uveitis, peripheral vasculitis, is also shown in Figure 9A and B, with respective histology shown in Figure 9C. Additionally, the OCT scan of the left eye revealed very small, white, hyperreflective spots on the epiretinal surface and within the nerve fiber layer (Figure 9B). Careful investigation reveals only sparse infiltration of inflammatory cells in the vitreous. In a rat eye with EAU (Figure 9D) inflammatory cells are distributed throughout all layers of the retina, as well as in the respective localizations in the nerve fiber and ganglion cell layers. Some cells also infiltrate the vitreous.

 doi:10.20944/preprints202512.1701.v1

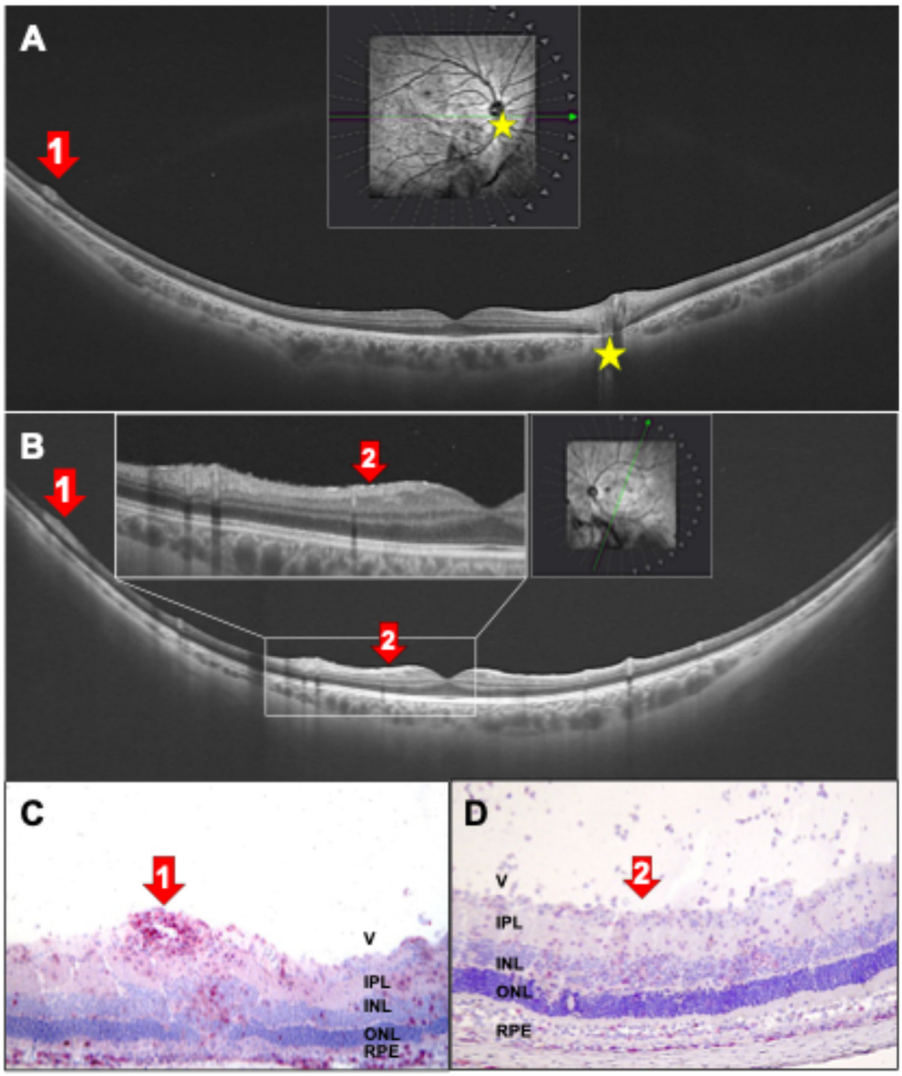

Figure 9. (A, B) Right (A) and left (B) eye of a 31-year-old patient with untreated intermediate uveitis with vasculitis (red arrows 1, yellow asterisk marks the papilla). (A-C) Red arrows 1: Peripheral perivascular swelling with vasculitis, rat EAU histology (C) with red staining of CD4+ cells. (B, D) Red arrows 2 show inflammatory cells on the retinal surface (B and D). V: vitreous, IPL: inner plexiform layer, INL: inner nuclear layer, ONL: outer nuclear layer, RPE: retinal pigment epithelium, Ch: choroid. (C) IRBP-immunized; (D) PDSAg-immunized.

4. Discussion

Human uveitis encompasses a wide range of clinical presentations and is classified as infectious or non-infections, anterior, intermediate or posterior uveitis with granulomatous, nodular or non-granulomatous/fibrinous inflammation. Very little is known about the immune pathomechanisms or the autoantigens of the immune response. Some retinal antigens have been identified as being recognized by peripheral lymphocytes of uveitis patients, such as retinal S-antigen, IRBP [8], cRALBP [9], and tyrosinase family proteins for Vogt-Koyanagi-Harada disease [19]. Conversely, some HLA molecules and polymorphisms of a few other molecules have been identified as being more or less strongly associated with certain uveitis entities. Finally, blame has been placed on the microbiome [20].

Similar, clinically classified presentations of uveitis may be manifestations of different entities. Noninfectious uveitis entities are sub-grouped according to their clinical presentations, as defined by slitlamp examination of the eye, fundoscopy, angiography of retinal and choroidal vessels, and OCT, which provides insight into the structure of the retina. OCT has led to a much better understanding of many eye diseases including uveitis. However, the resolution of the scans thus far only allows for an estimation of the inflammatory process in the retina, not a precise idea. In this manuscript, we

 doi:10.20944/preprints202512.1701.v1

analyzed immune cell migration into and infiltration of neuroretinal tissue in an EAU rat model, highlighting important analogies with OCT imaging findings in human patients with uveitis.

Although animal models of uveitis have their limitations, they have helped us to better understand the immunological pathomechanisms of the disease and develop therapies. EAU is a model of panuveitis with high inflammatory activity that leads to severe tissue damage within days. This contrasts with most human uveitis cases, which have a slower and less severe inflammatory. Nevertheless, the final tissue damage would be similar if no treatment were administered. Typical patterns of inflammatory activity include perivascular infiltrates (vasculitis), immune cell accumulation at the vitreoretinal interface/posterior hyaloid space (snowballs, snowbanks), and infiltration of the outer retinal layers by immune cells that migrated from the choroid.

Experimental uveitis is usually induced in certain strains of mice and rats. Although these experimental animals are genetically identical and are kept under the same environmental conditions, they exhibit variations in disease progression. Lewis rats exhibit individual differences in the clinical manifestations and histological findings of their uveitis.

The two major autoantigens for experimental autoimmune uveitis (EAU) in Lewis rats are retinal S-antigen (S-Ag) and IRBP [3]. Although rat EAU is defined as pan-uveitis, IRBP-induced EAU usually affects both the anterior and posterior segments, while S-Ag-induced uveitis affects the posterior segment more severely. The extracellular molecule IRBP shuttles vitamin A derivatives between photoreceptors and the RPE. S-Ag is an intracellular photoreceptor protein and taken up by RPE cells when the outer PR segments are phagocytosed. We have developed two uveitis models in Lewis rats, using two different antigen peptides for immunization, PDSAg derived from retinal S-Ag and R14 derived from IRBP. These antigens induce two distinct types of uveitis with respect of disease course and pathological findings.

PDSAg-induced uveitis has only one clinically visible course of inflammation, which resolves approximately three weeks after immunization. Around 28 days after immunization, new vessels grow from the choroid throughout the retina. We discovered that PDSAg-specific T helper cells secrete VEGF, which induces CNV. Suppressing T cells and their VEGF secretion inhibits CNV formation [6]. IRBP peptide R14-specific T cells do not produce VEGF or cause CNV growth. However, they can induce relapses of anterior uveitis that are visible clinically. These relapses depend on IFN-γ, as demonstrated by synchronized relapses following intraocular injection of this cytokine [13]. These clear differences between S-Ag and IRBP induced uveitis were only observed when the peptides, not the whole proteins, were used for immunization.

In rat EAU, the inflammatory cells are primarily monocytes and macrophages [21]. However, after the blood-eye barrier breaks down, all types of lymphocytes and leukocytes can invade the eye. The autoreactive CD4+ T cells themselves are not destructive to intraocular tissue; but they are the first to invade the eye. Only after a second local antigen encounter, they become reactivated and recruit inflammatory cells [12,22]. This three-day time lapse is the prodromal phase, which is sometimes experienced by patients with anterior uveitis.

T cells that are specific for S-Ag- and IRBP peptide also display differences in gene expression encoding different signal transduction pathways. Both antigen peptides induce Th1 and Th17 cells. However, PDSAg-specific T cells are more Th17-prone, with higher IL-17 secretion, while R14-specific T cells are more Th1 prone, with enhanced IFN-γ production. Gene array analysis of T cell lines with both specificities revealed differences in their expression of 29 genes and proteins. Except for VEGF, all are higher expressed in R14-specifc T cells [4,5,7].

While IFN-γ primes macrophages [23,24], IL-17 activates neutrophil granulocytes [25]. In the rat EAU models, we find T cells secreting either IFN-γ or IL-17 or coproducing both at the same time only in the eye, with changes in the population sizes during the course of inflammation. PDSAg-induced, clinically monophasic, but subclinically chronic uveitis, which results in CNV formation shows an increase in IL-17-producing T cells during the disease course. In contrast, in relapsing R14-induced EAU, IFN-γ-producing T cells increase and play a dominant role in inducing relapses [13]. These differences in the disease course could only be detected by using the two different peptides as

 doi:10.20944/preprints202512.1701.v1

antigens in the rat model. However, immunization with the respective complete antigen proteins, which include many different immunogenic epitopes, prevented this differentiation. In human patients we suspect that several antigens/epitopes are involved in the pathogenesis, especially in long-standing diseases where epitope-spreading occurs [3,26,27]. This results in a combination of several different immune responses with many phenotypes or a shift to a predominant immune response.

The phenomenon of T cell responses spreading to other epitopes of the same and other autoantigens over time has been observed in some peptide-immunized rats [3], and in spontaneous and experimentally induced uveitis in horses [27–29]. Co-immunization of rats with peptides PDSAg and R14 revealed dominance of the clinically monophasic, chronic PDSAg-mediated EAU and decreased relapses [7]. The same may be true for patients with intermediate and posterior uveitis, who tend to have a chronic rather than relapsing-remitting disease course. Unlike animal models, we expect a broader spectrum of human autoimmune T cell responses that will likely suppress some typical features, as demonstrated in the rat model following immunization with both autoantigen peptides and the subsequent suppression of the relapses.

As previously mentioned, the autoantigen specificity of the immune response in uveitis patients is unknown. However, in certain types of uveitis there may be a strong preference for one or a few autoantigens and their epitopes, similar to the situation in our rat model.

These different autoantigens may explain the differences in retinal damage observed after immunization with antigens like S-Antigen and IRBP. IRBP-induced uveitis tends to affect the anterior part of the eye more, possibly because IRBP mRNA has been found in the ciliary body [30]. In the posterior part of the eye, IRBP is present in the vitreous and the interphotoreceptor matrix, located between the retinal pigment epithelium (RPE) and the external limiting membrane. There, IRBP is secreted by photoreceptor rods and cones. For T cells to recognize it, IRBP must be taken up by antigen-presenting cells (APCs), degraded, and presented as peptides. Under physiological conditions, IRBP is taken up by RPE cells, where it is recycled but not degraded. This potentially excludes RPE cells from presenting IRBP peptides and delivering degraded IRBP to the choriocapillaris, as probably occurs with S-antigen. This may explain why infiltrating macrophages can destroy the outer segments of photoreceptors completely in IRBP/R14-induced EAU, while the RPE remains intact. Müller cells do not take up or degrade IRBP, thus disqualifying them as primary antigen-presenting cells [31]. It is not yet known which cells in the retina break down IRBP. However, since IRBP is free-floating in the interphotoreceptor matrix and elsewhere in the eye, it can easily be taken up by any cell in or entering the eye that qualifies as an APC, such as retinal microglia [32]. Enhanced antigen presentation and easy accessibility could also explain the earlier onset of IRBP-induced EAU compared to S-Ag/PDSAg-induced disease [3]. Microglia processes that extend to the outer plexiform layer can come into contact with retinal capillaries. This attracts IRBP-specific T cells, leading to increased infiltration between the two nuclear layers as can be observed in IRBP-induced disease [33]. This attracts IRBP-specific T cells, leading to increased infiltration between the two nuclear layers as can be observed in IRBP-induced disease.

The situation is different with S-Antigen. Upon phagocytosis of outer PR segments, S-Ag also appears in the retinal pigment epithelium (RPE), where it is degraded. Together with several growth factors, S-Ag fragments can be transported to the choriocapillaris [34], where they are taken up and presented by local macrophages. These macrophages can then attract lymphocytes from the vasculature to the RPE and into the retina. This process is followed by inflammatory cells that facilitate RPE destruction. RPE cells can also present antigen, but they usually express HLA class II molecules only under inflammatory conditions. Destruction of the RPE, which represents the outer blood-retina barrier, allows inflammatory cells to invade and severely damage the retinal architecture. In humans RPE destruction followed by scar formation leads to "white dots", which are often seen in chorioretinopathies during fundoscopic examination.

Treating rats with Met-RANTES 3 - 6 days after adoptive transfer only abrogated PDSAg-induced EAU, not R14-induced EAU [15]. As a receptor antagonist Met-RANTES competitively

 doi:10.20944/preprints202512.1701.v1

inhibits the binding of CCL2/RANTES to CCR1 and CCR5 but does not induce signaling. In EAU, activated autoreactive T cells enter the eye approximately three days before the onset of clinical disease (i.e., infiltration of inflammatory cells). When they recognize their respective antigen, they become reactivated and can recruit inflammatory cells to the inner eye a few days later [12]. Since PDSAg- and R14-specific T cells do not differ in their expression of respective chemokine receptors, we propose that Met-RANTES primarily acts on inflammatory cell infiltration rather than on T cells. In PDSAg-induced EAU, this occurs preferentially via the RPE, which is blocked by Met-RANTES binding (series record GSE19652 on the NCBI Gene Expression Omnibus webpage: http://www.ncbi.nlm.nih.gov/geo/) [4].

The secretion of VEGF by PDSAg-specific T cells leads to the growth of blood vessels from the choroid into the retina and further destroys the tissue. In rat EAU, we found that PDSAg- but not R14-specific rat T cells produce VEGF and therefore induce new blood vessel growth from the choroid into the retina [6]. Suppressing T cells also reduced new vessel growth, regardless of the extent of retinal destruction. This suggests that CNV formation in uveitis is primarily caused by T cell VEGF secretion rather than by RPE. Since we demonstrated VEGF secretion with human T cells as well, we propose that the sprouting of new blood vessels in the eyes of uveitis patients may also be caused by autoreactive T cells rather than by VEGF produced by the RPE or by macrophage secretion [6]. This notion is supported by the observation that choroidal neovascularization in human uveitis exhibits different characteristics than neovascularization resulting from other diseases, such as AMD, venous occlusion, and diabetes. For this reason, it has been named inflammatory choroidal neovascularization (iCNV) [35,36]. As in the animal model, immunosuppression reduces the recurrence of iCNV in humans, further supporting the idea that VEGF-dependent neovascularization is driven by T cells [37].

A limitation of this study, as well as a general limitation of animal models, is the difficulty of transferring the results to human disease. The two antigens and the two types of uveitis they induce are only two examples from the EAU rat model, but they demonstrate the differences in immune responses to specific antigens or epitopes and their effects on target tissues. The same may occur in patients, likely through a combination of immune responses rather than a single epitope specificity. Other autoantigens may result in different T cell types with additional characteristics, inducing different clinical manifestations and effects on ocular tissues than those shown here. Regardless of the autoantigen, inflammation patterns seem to repeat and resemble each other. This is evident in the close correspondence between human OCT and rat histology images.

The strength of this analysis lies in its detailed, tissue-level perspective on inflammation. There is an unmet need for a deeper understanding of the immunological basis of imaging signs in human uveitis. Currently, multimodal imaging is primarily used to make an exact diagnosis of uveitis and, to a lesser extent, to monitor therapeutic success. Identifying imaging criteria that indicate activity could make clinical control of uveitis activity far more precise. Thus far, OCT has primarily been used at the posterior pole, e.g., to assess the presence of cystoid macular edema (CME). With wide-field imaging, peripheral signs of active disease can be included in routine assessments and used to monitor the efficacy of immunomodulatory therapy. Ideally, relapses of uveitic inflammation could be reliably detected before visible clinical signs appear on the slit lamp and before harmful complications occur. Reliable imaging parameters for uveitis activity could serve as endpoints for evaluating the efficacy of uveitis treatments. These endpoints could solve the problem of irregular and unpredictable endpoints that lead to failed phase 3 trials [38]. The detailed insights of the rat histologies presented here could guide future basic science and clinical imaging studies.

Author Contributions: Conceptualization, BS and GW; methodology, BS and GW; validation, BS, ST and GW; formal analysis, GW; investigation, TG and GW; resources, TG and GW; data curation, TG and GW; writing—original draft preparation, BS, ST and GW; writing—review and editing, BS, TG, ST and GW; visualization, TG, BS and GW; supervision, GW; project administration, BS and GW; funding acquisition, GW. All authors have read and agreed to the published version of the manuscript.

 doi:10.20944/preprints202512.1701.v1

Funding: Rat histologies are from experiments funded by the Deutsche Forschungsgemeinschaft (DFG) SFB 217 and 571.

Institutional Review Board Statement: The study was conducted in accordance with the Declaration of Helsinki. The collection of clinical data including OCT imaging was approved by the Ethics Committee of the LMU Munich (protocol codes 24-0571 and 25-0390). All animal experiments were approved by the Review Board of the local government (Regierung von Oberbayern) and conformed to the ARVO Statement on the Use of Animals in Ophthalmic and Vision Research.

Informed Consent Statement: Informed consent was obtained from all subjects involved in the study.

Data Availability Statement: The original contributions presented in this study are included in the article. Further inquiries can be directed to the corresponding authors.

Acknowledgments: We thank Maximilian Gerhardt for the access to the ultrawidefield OCT device.

Conflicts of Interest: The authors declare no conflicts of interest.

Abbreviations

The following abbreviations are used in this manuscript:

CME: cystoid macular edema
CNV: choroidal neovascularization
cSLO: confocal scanning laser ophthalmoscope
EAU: experimental autoimmune uveitis
IRBP: interphotoreceptor retinoid-binding protein
OCT: optical coherence tomography
PDSAg: peptide derived from retinal S-antigen
PIC: punctate inner choroidopathy
RPE: retinal pigment epithelium
R14: peptide derived from IRBP
S-Ag: S-Antigen, retinal soluble antigen
SD-OCT: spectral-domain optical coherence tomography
SS-OCT: swept-source optical coherence tomography
VEGF: vascular endothelial growth factor

References

1. Jabs, D.A., R.B. Nussenblatt, and J.T. Rosenbaum, Standardization of uveitis nomenclature for reporting clinical data. Results of the First International Workshop. Am J Ophthalmol, 2005. **140**(3): p. 509-16.
2. Invernizzi, A., et al., Minimum Imaging Sets for Diagnosis, Activity Assessment, and Complications in Noninfectious Posterior Uveitis - Multimodal Imaging in Uveitis (MUV) Task Force Report 9. Am J Ophthalmol, 2025. **280**: p. 106-119.
3. Diedrichs-Möhring, M., C. Hoffmann, and G. Wildner, *Antigen-dependent monophasic or recurrent autoimmune uveitis in rats.* Int Immunol, 2008. **20**(3): p. 365-74.
4. von Toerne, C., et al., Effector T cells driving monophasic vs. relapsing/remitting experimental autoimmune uveitis show unique pathway signatures. Mol Immunol, 2010. **48**(1-3): p. 272-80.
5. Wildner, G. and U. Kaufmann, What causes relapses of autoimmune diseases? The etiological role of autoreactive T cells. Autoimmun Rev, 2013. **12**(11): p. 1070-5.
6. Diedrichs-Möhring, M., et al., A new small molecule for treating inflammation and chorioretinal neovascularization in relapsing-remitting and chronic experimental autoimmune uveitis. Invest Ophthalmol Vis Sci, 2014. **56**(2): p. 1147-57.
7. Diedrichs-Möhring, M., U. Kaufmann, and G. Wildner, The immunopathogenesis of chronic and relapsing autoimmune uveitis - Lessons from experimental rat models. Prog Retin Eye Res, 2018. **65**: p. 107-126.

 doi:10.20944/preprints202512.1701.v1

8. de Smet, M.D., et al., Cellular Immune Responses of Patients with Uveitis to Retinal Antigens and Their Fragments. American Journal of Ophthalmology, 1990. **110**(2): p. 135-142.
9. Deeg, C.A., et al., CRALBP is a highly prevalent autoantigen for human autoimmune uveitis. Clin Dev Immunol, 2007. **2007**: p. 39245.
10. Nussenblatt, R.B., et al., *Cyclosporin a. Inhibition of experimental autoimmune uveitis in Lewis rats.* The Journal of Clinical Investigation, 1981. **67**(4): p. 1228-1231.
11. Wildner, G. and S.R. Thurau, Cross-reactivity between an HLA-B27-derived peptide and a retinal autoantigen peptide: a clue to major histocompatibility complex association with autoimmune disease. Eur J Immunol, 1994. **24**(11): p. 2579-85.
12. Thurau, S.R., et al., The fate of autoreactive, GFP+ T cells in rat models of uveitis analyzed by intravital fluorescence microscopy and FACS. Int Immunol, 2004. **16**(11): p. 1573-82.
13. Kaufmann, U., M. Diedrichs-Möhring, and G. Wildner, Dynamics of intraocular IFN-γ, IL-17 and IL-10-producing cell populations during relapsing and monophasic rat experimental autoimmune uveitis. PLoS One, 2012. **7**(11): p. e49008.
14. Diedrichs-Möhring, M., et al., Intraocular DHODH-inhibitor PP-001 suppresses relapsing experimental uveitis and cytokine production of human lymphocytes, but not of RPE cells. J Neuroinflammation, 2018. **15**(1): p. 54.
15. Diedrichs-Möhring, M., et al., The effect of the CC chemokine receptor antagonist Met-RANTES on experimental autoimmune uveitis and oral tolerance. J Neuroimmunol, 2005. **164**(1-2): p. 22-30.
16. Spaide, R.F., N. Goldberg, and K.B. Freund, Redefining multifocal choroiditis and panuveitis and punctate inner choroidopathy through multimodal imaging. Retina, 2013. **33**(7): p. 1315-24.
17. Agrawal, R., et al., Morphometric features on enhanced depth imaging optical coherence tomography scans in idiopathic posterior uveitis or panuveitis. Int Ophthalmol, 2018. **38**(3): p. 993-1002.
18. Wetzig, R.P., et al., Clinical and immunopathological studies of pars planitis in a family. Br J Ophthalmol, 1988. **72**(1): p. 5-10.
19. Yamaki, K., et al., Tyrosinase family proteins are antigens specific to Vogt-Koyanagi-Harada disease. J Immunol, 2000. **165**(12): p. 7323-9.
20. Abramowicz, S., *Genetic polymorphisms and uveitis.* Acta Ophthalmologica, 2025. **103**(S284).
21. Robertson, M., et al., Neutralizing Tumor Necrosis Factor-α Activity Suppresses Activation of Infiltrating Macrophages in Experimental Autoimmune Uveoretinitis. Investigative Ophthalmology & Visual Science, 2003. **44**(7): p. 3034-3041.
22. Prendergast, R.A., et al., T cell traffic and the inflammatory response in experimental autoimmune uveoretinitis. Invest Ophthalmol Vis Sci, 1998. **39**(5): p. 754-62.
23. Simpson, D.S., et al., Interferon-gamma primes macrophages for pathogen ligand-induced killing via a caspase-8 and mitochondrial cell death pathway. Immunity, 2022. **55**(3): p. 423-441.e9.
24. Schwarzenberger, P., et al., Requirement of Endogenous Stem Cell Factor and Granulocyte-Colony-Stimulating Factor for IL-17-Mediated Granulopoiesis1. The Journal of Immunology, 2000. **164**(9): p. 4783-4789.
25. Griffin, G.K., et al., IL-17 and TNF-α sustain neutrophil recruitment during inflammation through synergistic effects on endothelial activation. J Immunol, 2012. **188**(12): p. 6287-99.
26. Garip, A., et al., Uveitis in a patient treated with Bacille-Calmette-Guérin: possible antigenic mimicry of mycobacterial and retinal antigens. Ophthalmology, 2009. **116**(12): p. 2457-62.e1-2.
27. Deeg, C.A., et al., Uveitis in horses induced by interphotoreceptor retinoid-binding protein is similar to the spontaneous disease. European Journal of Immunology, 2002. **32**(9): p. 2598-606.
28. Deeg, C.A., et al., Immune responses to retinal autoantigens and peptides in equine recurrent uveitis. Invest Ophthalmol Vis Sci, 2001. **42**(2): p. 393-8.
29. Deeg, C.A., et al., *The uveitogenic potential of retinal S-antigen in horses.* Invest Ophthalmol Vis Sci, 2004. **45**(7): p. 2286-92.
30. Salvador-Silva, M., et al., Retinoid processing proteins in the ocular ciliary epithelium. Mol Vis, 2005. **11**: p. 356-65.

 doi:10.20944/preprints202512.1701.v1

31. Hollyfield, J.G., et al., Endocytosis and degradation of interstitial retinol-binding protein: differential capabilities of cells that border the interphotoreceptor matrix. J Cell Biol, 1985. **100**(5): p. 1676-81.
32. Gonzalez-Fernandez, F., *Interphotoreceptor retinoid binding protein; myths and mysteries.* J Ophthalmic Vis Res, 2012. **7**(1): p. 100-4.
33. Dixon, M.A., et al., The Contribution of Microglia to the Development and Maturation of the Visual System. Front Cell Neurosci, 2021. **15**: p. 659843.
34. Strauss, O., *The retinal pigment epithelium in visual function.* Physiol Rev, 2005. **85**(3): p. 845-81.
35. Servillo, A., et al., Inflammatory choroidal neovascularization: An evidence-based update. Surv Ophthalmol, 2025. **70**(3): p. 451-466.
36. Bottazzi, L., et al., Choroidal neovascularization secondary to punctate inner choroidopathy vs myopia: clinical outcomes after 1-year of treatment. Graefes Arch Clin Exp Ophthalmol, 2025. **263**(7): p. 1859-1865.
37. Airaldi, M., et al., Immunomodulatory Treatment Versus Systemic Steroids in Inflammatory Choroidal Neovascularization Secondary to Idiopathic Multifocal Choroiditis. Am J Ophthalmol, 2024. **262**: p. 62-72.
38. Jabs, D.A., et al., The Conundrum of Clinical Trials for the Uveitides: Appropriate Outcome Measures for One Treatment Used in Several Diseases. Epidemiol Rev, 2022. **44**(1): p. 2-16.